Exposure duration modulates the response of Caribbean corals to global change stressors

Hannah E. Aichelman,[1,2*] **Colleen B. Bove**,[1,3] **Karl D. Castillo**,[2,3] **Jessica M. Boulton**,[2] **Alyssa C. Knowlton**,[2] **Olivia C. Nieves**,[1] **Justin B. Ries**,[4] **Sarah W. Davies**[1,2,4*]

[1]Department of Biology, Boston University, Boston, Massachusetts
[2]Department of Marine Sciences, University of North Carolina at Chapel Hill, Chapel Hill, North Carolina
[3]Environment, Ecology, and Energy Program, University of North Carolina at Chapel Hill, Chapel Hill, North Carolina
[4]Department of Marine and Environmental Sciences, Northeastern University, Boston, Massachusetts

Abstract

Global change, including rising temperatures and acidification, threatens corals globally. Although bleaching events reveal fine-scale patterns of resilience, traits enabling persistence under global change remain elusive. We conducted a 95-d controlled-laboratory experiment investigating how duration of exposure to warming (~28, 31°C), acidification (pCO_2 ~ 343 [present day], ~663 [end of century], ~3109 [extreme] μatm), and their combination influences physiology of reef-building corals (*Siderastrea siderea*, *Pseudodiploria strigosa*) from two reef zones on the Belize Mesoamerican Barrier Reef System. Every 30 d, net calcification rate, host protein and carbohydrate, chlorophyll *a*, and symbiont density were quantified for the same coral individual to characterize acclimation potential under global change. Coral physiologies of the two species were differentially affected by stressors and exposure duration was found to modulate these responses. *Siderastrea siderea* exhibited resistance to end of century pCO_2 and temperature stress, but calcification was negatively affected by extreme pCO_2. However, *S. siderea* calcification rates remained positive after 95 d of extreme pCO_2 conditions, suggesting acclimation. In contrast, *P. strigosa* was more negatively influenced by elevated temperatures, which reduced most physiological parameters. An exception was nearshore *P. strigosa*, which maintained calcification rates under elevated temperature, suggesting local adaptation to the warmer environment of their natal reef zone. This work highlights how tracking coral physiology across various exposure durations can capture acclimatory responses to global change stressors.

Since the Industrial Revolution, anthropogenic activities have increased the partial pressure of atmospheric carbon dioxide (pCO_2), causing atmospheric warming of ~0.6°C (Pörtner et al. 2019). As atmospheric temperatures increase, so do sea surface temperatures (SSTs) (Pörtner et al. 2019). Increasing pCO_2 has also caused surface ocean pH to decrease by 0.017–0.027 units per decade since the 1980s (e.g., Pörtner et al. 2019). Warming and acidification have impacted organisms across the globe, as thermal niches shift and habitats rapidly change (Morley et al. 2018; Pörtner et al. 2019). The negative effects of global climate change are predicted to strengthen and, under the Intergovernmental Panel on Climate Change's (IPCC) most extreme emissions scenario (RCP8.5), oceans are expected uptake 5–7 times more heat and decrease by 0.3 pH units by 2100 (Van Vuuren et al. 2011; Pörtner et al. 2019).

Coral reefs are valuable economic and ecological resources (Costanza et al. 2014) that are vulnerable to ocean warming and acidification. The high biodiversity of coral reefs depends on the obligate symbiosis between corals and their symbiotic algae (Symbiodiniaceae, previously genus *Symbiodinium*; LaJeunesse et al. 2018). This symbiosis is sensitive to thermal anomalies and, because tropical reef-building corals live within 1°C of their upper thermal limit, small SST increases can result in bleaching (breakdown of symbiosis) and ultimately mortality if symbionts fail to repopulate the coral host. These coral bleaching events are occurring with increasing frequency and severity as SSTs continue to rise (Hughes et al. 2017).

Ocean acidification alters seawater carbonate chemistry (Doney et al. 2009) by reducing seawater pH, carbonate ion concentration ($[CO_3^{2-}]$), and the saturation state of seawater with respect to aragonite (Ω_{arag})—which can make it challenging for corals to build their aragonite skeletons (Doney

*Correspondence: haich@bu.edu and daviessw@bu.eu

Additional Supporting Information may be found in the online version of this article.

et al. 2009). Laboratory experiments have shown that projected acidification conditions can have negative (Horvath et al. 2016 [888–940 μatm]; reviewed in Hoegh-Guldberg et al. 2007), neutral (Reynaud et al. 2003 [760 μatm]) threshold (Ries et al. 2010 [409–2856 μatm]), and parabolic (Castillo et al. 2014 [324–2553 μatm]) impacts on coral calcification, while in situ manipulative field experiments have yielded more negative outcomes (Albright et al. 2018; Kline et al. 2019). The direction and magnitude of coral calcification responses to acidification are influenced by numerous factors, including species-level differences (Okazaki et al. 2017; Bove et al. 2019), differences in the ability to regulate calcifying fluid chemistry (Ries 2011; Liu et al. 2020; Guillermic et al. 2021), CO_2-induced fertilization of photosynthesis (Guillermic et al. 2021), gonochoric colony sex (Holcomb et al. 2012), experimental duration (Kline et al. 2019), co-occurring thermal stress (Kroeker et al. 2013), boundary layer limitation of proton flux (Jokiel 2011), heterotrophy (Towle et al. 2015), and biomass energy utilization (Wall et al. 2017). Calcification in response to temperature stress is similarly complicated by a number of factors. For example, calcification rates of corals have been shown to respond parabolically to temperature, with trends varying across species (Edmunds 2005). Additional complexities have been linked to life history and seasonality (Kornder et al. 2018). Energetic reserves are critical to coral health and resistance to stressors and have been associated with bleaching susceptibility (Anthony et al. 2009; Levas et al. 2018) and whether a bleaching event will lead to mortality (Grottoli et al. 2006; Anthony et al. 2009). Additionally, a coral's response to thermal stress—like their response to acidification—can be mediated by heterotrophy (Grottoli et al. 2006; Aichelman et al. 2016).

Fewer studies consider the interactions of temperature and acidification stress, and these studies have similarly produced variable results. Although some research finds stronger negative effects of elevated temperature compared to acidification on calcification (Schoepf et al. 2013; Anderson et al. 2019) and survivorship (Anderson et al. 2019), others have shown additive effects of the two stressors (Rodolfo-Metalpa et al. 2011; Edmunds et al. 2012; Agostini et al. 2013; Horvath et al. 2016). The response of the coral holobiont to environmental stress varies by stressor, and also by species. Such species-level differences have been observed in coral calcification under crossed temperature and acidification stress (Okazaki et al. 2017; Bove et al. 2019) and recovery of energetic reserves through time after bleaching (Levas et al. 2018). Additionally, spatial scale can play a role in response to environmental stress, with differential stress tolerance observed across populations along a reef system (Dixon et al. 2015), between reef zones (Castillo et al. 2012; Kenkel et al. 2013*a*), and between tidal pools (Bay and Palumbi 2014), illustrating that adaptation and/or acclimation to fine scale environmental differences can play a role in determining stress response. Therefore, a more complete understanding of the interactions of environmental stressors necessitates investigations of multiple species from different populations in response to multiple stressors across longer timescales with a focus on holobiont physiology.

Considering how duration of stress exposure affects the coral holobiont is critical (McLachlan et al. 2020), but this pursuit is complicated by the difficulty of executing long-term laboratory experiments. However, several studies have been conducted for ~90 d or more, revealing patterns of stress and resilience. For example, acidification (1050 μatm pCO_2) caused rapid, species-specific alterations of calcifying fluid chemistry in four coral and two calcifying algae species that remained for 1 yr (Comeau et al. 2019). Castillo et al. (2014) showed calcification responses to elevated pCO_2 varied with exposure duration, with *S. siderea* calcification under moderate pCO_2 (604 μatm) increasing between 0 and 60 d and decreasing between 60 and 90 d. Additionally, Levas et al. (2018) tracked corals for 11 months following experimental bleaching and found interspecific differences in recovery. *Porites divaricata* initially catabolized lipids and decreased calcification but recovered within 11 months, while *P. astreoides* recovered within 1.5 months after increasing feeding and symbiont nitrogen uptake (Levas et al. 2018). In summary, tracking coral physiology through time provides valuable insights into how corals respond to short-, moderate-, and long-term stress.

Here, two ecologically important reef-building coral species (*Siderastrea siderea* and *Pseudodiploria strigosa*) from two reef zones with distinct thermal environments (forereef and nearshore; Baumann et al. 2016) of the Belize Mesoamerican Barrier Reef System (MBRS) were maintained under a fully crossed pCO_2 (~343 μatm [present day], ~663 μatm [end of century], ~3109 μatm [extreme]), and temperature (~28, 31°C) 95-d experiment. Control and elevated temperature treatments correspond to present-day mean annual temperature from the collection sites on the MBRS (Castillo et al. 2012; Baumann et al. 2016) and projected end of century annual mean temperature for this region (IPCC 2013), respectively. End of century pCO_2 is based on the RCP6 emissions scenario, and extreme pCO_2 is a projection for the year 2500 under RCP8.5 (IPCC 2013) and is intended to test a coral's response to extreme acidification. To characterize the species' responses to projected global change, holobiont physiology of each colony was monitored approximately every 30 d (exposure duration: 0–30 d = T_0 – T_{30} = short-term, 30–60 d = T_{30} – T_{60} = moderate-term, 60–95 d = T_{60} – T_{95} = long-term), including metrics for coral host (calcification rate, protein, carbohydrates) and algal symbiont (symbiont cell density, chlorophyll *a*). This work elucidates the impact of exposure duration on corals' acclimatory response to global change stressors.

Materials and methods

Coral collection and experimental design

The experiment presented here was run in parallel with that published by Bove et al. (2019); therefore, experimental

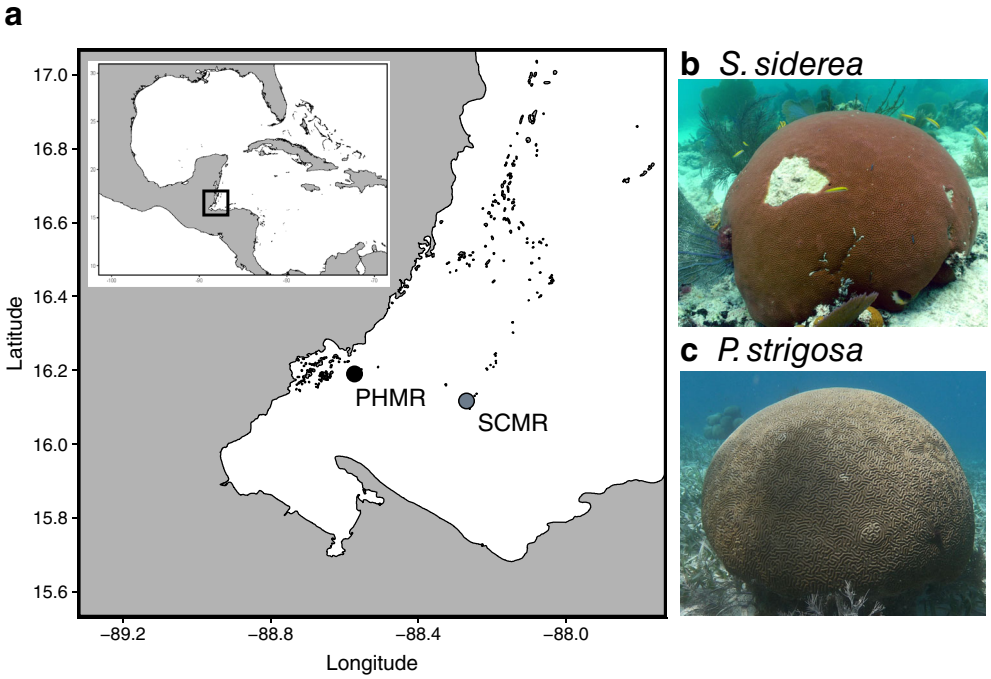

Fig. 1. (**a**) Map of forereef (SCMR = Sapodilla Cayes Marine Reserve) and nearshore (PHMR = Port Honduras Marine Reserve) coral collection sites on the Belize Mesoamerican Barrier Reef System. (**b**) Example of *Siderastrea siderea* (photo credit: K.D. Castillo). (**c**) Example of *Pseudodiploria strigosa* (photo credit: H.E. Aichelman).

design and culturing conditions are similar to those presented therein. However, our study used different coral colonies and only two species (instead of four). Experimental timing is staggered by 30 d between the two experiments; for comparison, T_0 here corresponds to "pre-acclimation period" in Bove et al. (2019). This difference in timing is intentional because we wanted to observe the effects of the initial exposure period, while Bove et al. (2019) treated this as "pre-acclimation" and excluded this experimental interval. Methods specific to this experiment are presented below with additional details in the Supporting Information.

Three colonies of *Siderastrea siderea* and three colonies of *Pseudodiploria strigosa* were collected from a nearshore and forereef site along the southern Belize MBRS (Fig. 1, Supporting Information). All colonies were transported to Northeastern University's Marine Science Center in Nahant, Massachusetts and fragmented into 24 pieces. One forereef *P. strigosa* colony did not survive fragmentation, leaving three genotypes for nearshore and forereef *S. siderea*, three genotypes for nearshore *P. strigosa*, but only two genotypes for forereef *P. strigosa*. We acknowledge that replication across reef zone is limited; however, sample size was restricted by permitting, space was limited within experimental tanks, as well as the large colony size and number of fragments needed to consider genet-level coral physiology through time. After fragmentation, corals recovered for 23 d in natural flow-through seawater (5 μm-filtered seawater obtained from Massachusetts Bay) maintained at 28.2 $\pm$ 0.5°C and ~500 μatm pCO_2. Following recovery, temperature and pCO_2 were incrementally adjusted over 20 d until target treatments were achieved. The six experimental treatments consisted of a full factorial design of two temperatures (target: 28, 31°C) and three pCO_2 levels (target: 400, 700, 2800 μatm). In order to capture genotype-specific responses through time, four replicate coral fragments per genotype were represented in each of the six treatments, and each treatment was replicated in three 42 L acrylic tanks on a 10:14 h light:dark cycle (full spectrum LED lights; Euphotica, 120 W, 20,000 K) with PAR of ~300 μmol photons m^{-2} s^{-1} (consistent with Castillo et al. 2014). Coral fragments were fed a combination of ~6 g frozen adult *Artemia* sp. and 250 mL newly hatched live *Artemia* sp. (500 mL^{-1}) every other day and maintained in treatment conditions for 95 d or until preservation.

Experimental conditions were maintained similarly to Bove et al. (2019). Temperature, salinity, and pH were measured in all tanks every few days (n = 40 total) and water samples for total alkalinity (TA) and dissolved inorganic carbon (DIC) were collected a total of seven times throughout the experimental period. TA and DIC were measured using a VINDTA 3C (Marianda Corporation, Kiel, Germany) calibrated with certified Dickson Laboratory standards for seawater CO_2 measurements (Scripps Institution of Oceanography; San Diego, California). Temperature, salinity, TA, and DIC were used to calculate all carbonate system parameters using CO_2SYS

(Pierrot et al. 2006) with Roy et al. (1993) carbonic acid constants K_1 and K_2, the Mucci (1983) value for the stoichiometric aragonite solubility product, and an atmospheric pressure of 1.015 atm. All measured and calculated seawater parameters are reported in Figs. S1, S2, and Tables S1, S2. Cumulative average (±SE) pCO_2 and temperature throughout the 95-d experimental period (n = 20–21) were 298 ± 27 μatm, 28.0 ± 0.04°C (present day pCO_2, 28°C); 388 ± 25 μatm, 31.1 ± 0.04°C (present day pCO_2, 31°C); 663 ± 13 μatm, 28.0 ± 0.06°C (end of century pCO_2, 28°C); 662 ± 28 μatm, 31.0 ± 0.03°C (end of century pCO_2, 31°C); 2973 ± 125 μatm, 28.1 ± 0.02°C (extreme pCO_2, 28°C); 3245 ± 154 μatm, 30.7 ± 0.06°C (extreme pCO_2, 31°C).

Coral host and symbiont physiology

Coral host and symbiont physiological measurements were taken at each of the four time points (T_0, T_{30}, T_{60}, T_{95}). Net calcification rates were estimated in triplicate for each fragment using the buoyant weight technique (Davies 1989) and normalized to surface area. A subset of fragments from both species was used to confirm the relationship between buoyant weight and dry weight (as in Bove et al. 2019, details in Supporting Information). Growing surface area was quantified in triplicate from photos taken at each timepoint using ImageJ software (Rueden et al. 2017). The same surface area values of each coral fragment were used to normalize all host and symbiont physiological parameters within a time point. Additionally, at each time point, a fragment of each colony was removed from each treatment, flash frozen in liquid nitrogen, and stored at −80°C until processing, when fragments were airbrushed to remove host tissue and symbiont cells. Tissue slurries were homogenized and centrifuged to separate coral tissue and symbiont fractions for physiological assays. Fragments were frozen approximately every 30 d, but the actual number of days from T_0 to sampling were 36 (T_0 to T_{30}), 63 (T_0 to T_{60}), and 92 (T_0 to T_{95}). Because corals were frozen on the same day for each time point, there was no need to correct for the number of days in experimental treatment for physiological metrics other than calcification rate.

Total coral host protein content was quantified from host tissue slurry using a bicinchoninic acid protein assay following manufacturer's instructions. Total host carbohydrates were quantified using the phenol-sulfuric acid method (as in Masuko et al. 2005), which measures all monosaccharides, including glucose—the major photosynthate translocated from symbiont to coral (Burriesci et al. 2012). Symbiont cell density was quantified using the hemocytometer method (as in Rodrigues and Grottoli 2007). Symbiont photosynthetic pigments (chlorophyll *a*, abbreviated Chl *a*) were quantified spectrophotometrically following Marchetti et al. (2012). See Supporting Information for additional details.

Statistical analyses

Statistical differences between experimental treatments were tested using an ANOVA (*aov*) with fixed effects of temperature and pCO_2, and post-hoc pairwise comparisons were assessed using Tukey's HSD tests (Table S7). Temperature and pCO_2 data were log-transformed if necessary to meet assumptions of normality, which was assessed via a Shapiro–Wilk Test (*shapiro.test*). The results of statistical differences between treatments are reported in Table S7 as well as Figs. S1 and S2. Coral physiological data were assessed using a series of linear mixed effects models (*lmer*) for each species and individual physiological parameter (including fixed effects of time, temperature, pCO_2, and reef zone) using a forward model selection method (Supporting Information). A random effect of genotype was included in all models to account for physiological variation across genotypes. Physiological data were transformed to meet assumptions of normality for ANOVAs when necessary, including several parameters for *P. strigosa* (symbiont density [cube root], Chl *a* [square root], carbohydrate [square root]) and *S. siderea*: symbiont density [log], Chl *a* [cube root], carbohydrates [square root]). *Siderastrea siderea* calcification rates did not meet assumptions of normality despite transformations; therefore, a generalized additive model for location scale and shape with a Weibull distribution (*gamlss* package; Rigby and Stasinopoulos 2005) was fit using the same forward model selection method (Supporting Information). Model results are reported with summary statistics in Table S3. Significant post-hoc pairwise comparisons from linear mixed effects models were assessed using Tukey's HSD tests implemented in the *lsmeans* function (reported in Table S4).

Principal components analyses (PCA) were constructed using the *FactoMineR* package (Lê et al. 2008) to assess how overall physiologies were modulated through time for each species. Significance of each factor in the PCA was assessed using PERMANOVA, via the *adonis* function in the *vegan* package (Oksanen 2011). Statistics for all *adonis* tests are reported in Table S5.

Correlation matrices of all host and symbiont physiological parameters for both species through time were built using the *corrplot* function with a significance threshold of $p = 0.05$. Impacts of temperature and pCO_2 on host and symbiont physiology of only *P. strigosa* were assessed via linear regression modeling, as no noteworthy correlations were found for *S. siderea*. To estimate significance of predictors and their interactions, increasingly parsimonious, nested linear models (using *lmer*) were compared with likelihood ratio tests. Conditional *R*-squared values, accounting for both fixed and random effects, of regressions were determined using the *r.squaredGLMM* function in the *MuMIn* package. Summary statistics for all linear regressions are reported in Table S6. All raw data and code associated with analyses presented here are stored in a Github repository at the following link: https://github.com/hannahaichelman/TimeCourse_Physiology and

are additionally hosted on Zenodo (doi: 10.5281/zenodo.4914428). All statistical analyses used R version 4.0.1 (R Core Team 2017).

Results

Holobiont physiology through time

Siderastrea siderea holobiont physiology (calcification rate, host protein and carbohydrate, Chl *a*, symbiont density) clustered more strongly by pCO_2 than by temperature (Fig. 2a–c). There was an apparent, but not statistically significant, effect of pCO_2 on holobiont physiology after short-term exposure (T_{30}, $p = 0.054$; Fig. 2a), and this effect became significant through time (T_{95}, $p = 0.002$; Fig. 2c). At T_{95}, the interaction of pCO_2 and temperature was also significant ($p = 0.001$; Fig. 2c). Calcification, symbiont density, and Chl *a* PCA loadings discriminate between clusters of fragments in extreme pCO_2 and other acidification treatments (Fig. 2a-c). Comparing PCAs in Fig. 2a–c with individual physiological results (Figs. 4a,c and 5a,c) demonstrates that pCO_2 significantly reduced *S. siderea* calcification, symbiont density, and Chl *a*, but did not have a significant effect on host carbohydrates or protein. Reef zone did not have a significant effect on *S. siderea* holobiont physiology for any exposure duration (Fig. 2a–c).

Holobiont physiology of *P. strigosa* clustered more strongly by temperature than by pCO_2, especially after long-term exposure (T_{95}; Fig. 2d–f). At T_{60}, there was a significant effect of pCO_2 on holobiont physiology ($p = 0.029$; Fig. 2e). However, at T_{95} pCO_2 was no longer significant, and only temperature had a significant effect ($p = 0.045$; Fig. 2f). Additionally, the interaction of reef zone and temperature had a marginally significant effect on holobiont physiology after long-term exposure (T_{95}; $p = 0.053$; Fig. 2f). Comparing PCAs in Fig. 2d–f with results from individual physiological parameters (Figs. 4b,d and 5b,d) shows that elevated temperature resulted in consistent negative effects on all physiological parameters.

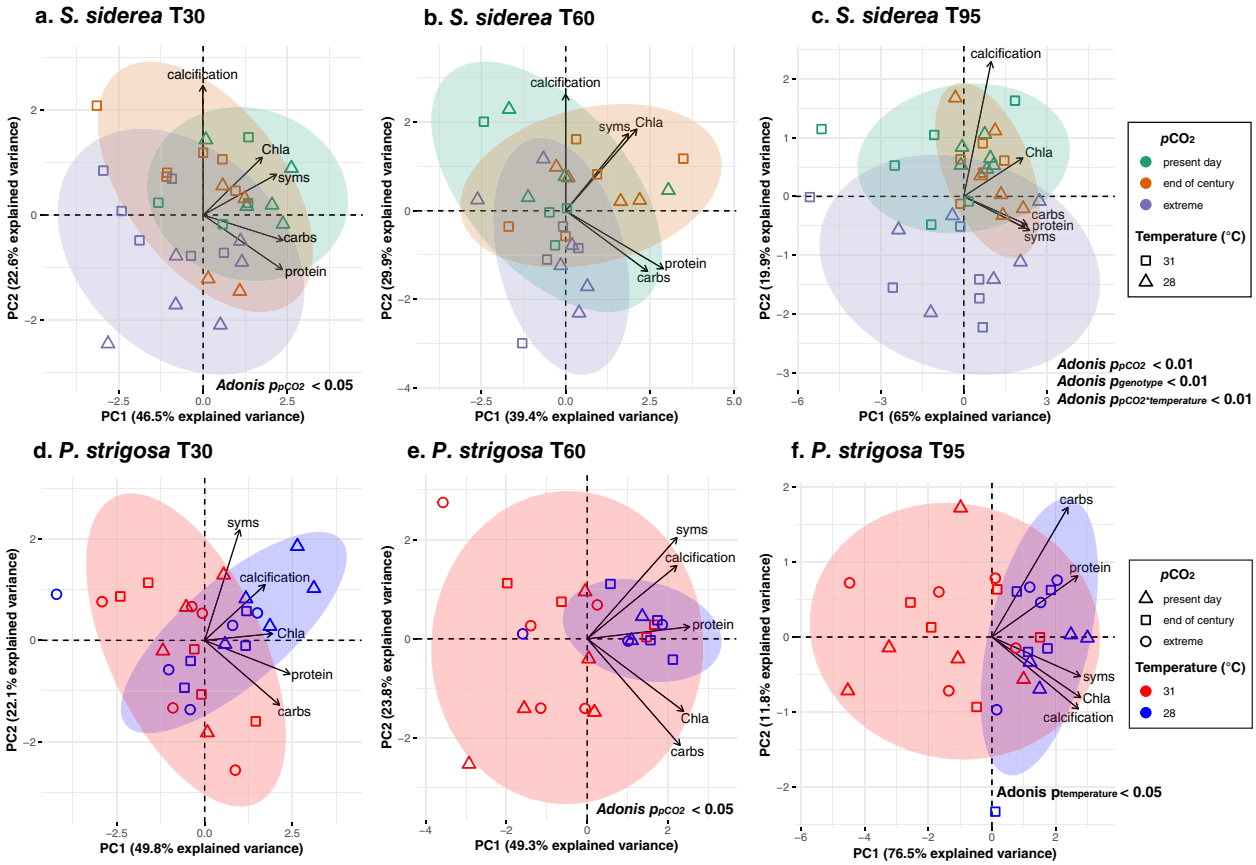

Fig. 2. Influence of temperature, pCO_2, and exposure duration on holobiont physiology. Principal components analyses (PCA) of log-transformed holobiont physiological data, including total carbohydrate (carbs; mg cm^{-2}), total protein (protein; mg cm^{-2}), symbiont density (syms; cells cm^{-2}), chlorophyll *a* (Chl *a*; μg cm^{-2}), and calcification (mg cm^{-2} d^{-1}) for *Siderastrea siderea* (**a**–**c**) and *Pseudodiploria strigosa* (**d**–**f**). Colors represent pCO_2 for *S. siderea* (**a**–**c**: green = present day, orange = end of century, purple = extreme) and temperature for *P. strigosa* (**d**–**f**: red = 31°C, blue = 28°C). Shapes represent temperature for *S. siderea* (**a**–**c**: square = 31°C, triangle = 28°C) and pCO_2 for *P. strigosa* (**d**–**f**: triangle = present day, square = end of century, circle = extreme). Points represent an individual coral fragment's physiology at each time point (**a**, **d** = short-term [T_{30}], **b**, **e** = moderate-term [T_{60}], **c**, **f** = long-term [T_{95}]). Only individuals with data for all five parameters at each time point were included. The *x*- and *y*-axes indicate variance explained (%) by the first and second principle component, respectively.

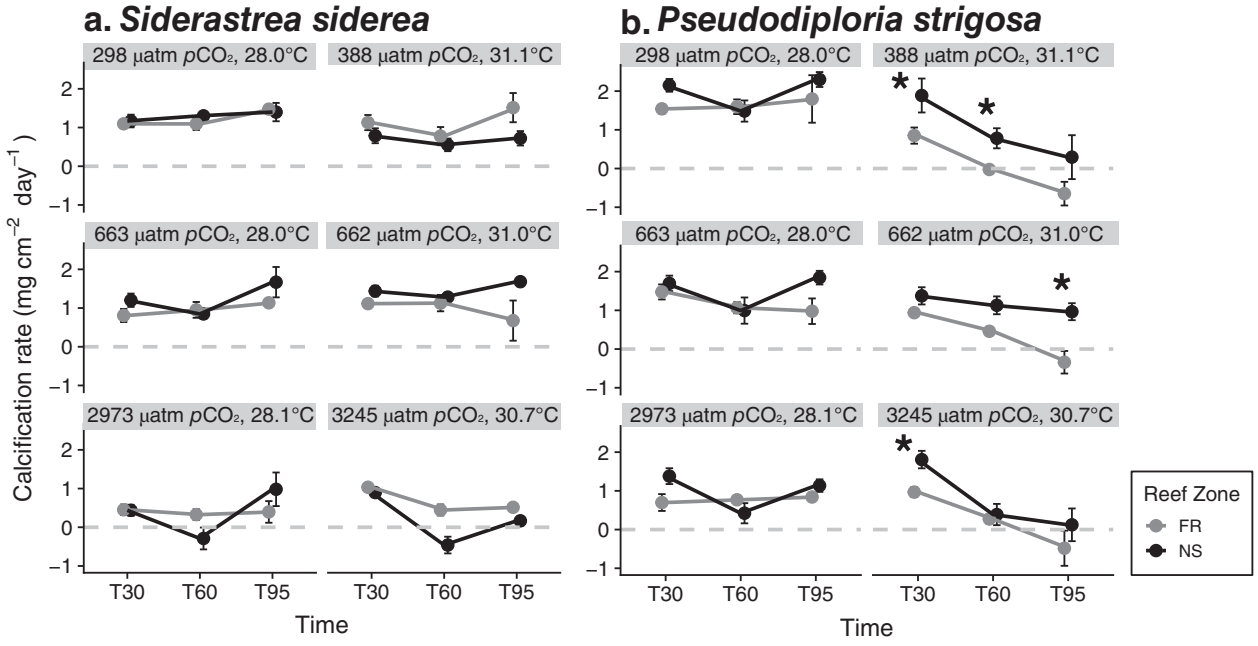

Fig. 3. *Siderastrea siderea* (**a**) and *Pseudodiploria strigosa* (**b**) net calcification rate (mg cm^{-2} d^{-1}) at each experimental time point (short-term = T_{30}; moderate-term = T_{60}; long-term = T_{95}). Facets represent the six treatments and are labeled with average pCO_2 and temperature for the experiment duration (pCO_2: Present day [top row], end of century [middle row], extreme [bottom row]; temperature: Control [left column], elevated [right column]). Within a facet, data are separated by reef zone (FR = forereef; NS = nearshore). Points represent mean calcification rates since the previous time point (i.e., T_{30} represents calcification between T_0 and T_{30}). Asterisks indicate significant ($p < 0.05$) differences in calcification rates between reef zones within a time point. Error bars represent standard error. For (**a**), each data point represents three colonies. For (**b**), each forereef point represents 2 colonies and each nearshore point represents 3 colonies, except extreme pCO_2/28°C treatment at T_{60} and T_{95}, where one forereef colony is represented due to mortality. For both (**a**) and (**b**), n = 1–3 fragments/colony depending on time point (T_{30} $n = 3$, T_{60} $n = 2$, and T_{90} $n = 1$). Although there are exceptions due to mortality, sample size for each point should therefore be: T_{30} $n = 9$, T_{60} $n = 6$, and T_{90} $n = 3$ (degrees of freedom reported in Table S3).

Effects of temperature and pCO_2 stress on calcification

Siderastrea siderea net calcification rates were clearly influenced by pCO_2 and were significantly reduced under extreme pCO_2 relative to present day pCO_2 ($p = 0.002$; Fig. 3a). However, end of century pCO_2 did not significantly reduce *S. siderea* net calcification relative to present day pCO_2 ($p = 0.4$). Additionally, *S. siderea* net calcification was significantly reduced at T_{90} relative to T_{30} ($p = 0.02$). Neither temperature treatment nor reef zone significantly altered net calcification rates. For this and all remaining individual physiological parameters, full model outputs (estimate, standard error, *T*-value, etc.) are reported in Table S3, and post-hoc pairwise comparisons are reported in Table S4.

Pseudodiploria strigosa net calcification rates were significantly negatively affected by pCO_2 ($p < 0.001$; Fig. 3b), and when compared to present day pCO_2 calcification rates were reduced under end of century ($p = 0.02$) and extreme pCO_2 ($p < 0.001$). Calcification rates were also reduced at elevated temperature (31°C) relative to control conditions ($p < 0.001$), and nearshore corals exhibited higher net calcification rates than forereef corals ($p = 0.04$). A significant interaction of temperature and experimental duration was detected for *P. strigosa* calcification rates ($p < 0.001$), with calcification decreasing between T_{30} and T_{60} under control and elevated temperatures ($p < 0.05$); however, these reductions were not detectable after moderate- and long-term exposure (T_{60} and T_{95}). When considering the full duration of the experiment (T_0 to T_{95}), *P. strigosa* net calcification rates were lower under elevated, but not control temperatures (Fig. 3b). Additionally, a significant interaction between reef zone and temperature on *P. strigosa* calcification rate was detected ($p = 0.03$), with elevated temperatures more negatively influencing calcification of forereef corals than nearshore corals ($p = 0.02$). Lastly, there was a significant interaction between temperature and pCO_2 on *P. strigosa* calcification rates ($p < 0.001$). Specifically, there were no significant differences in *P. strigosa* calcification rates among pCO_2 treatments under elevated temperatures, but calcification rates in control temperatures were significantly reduced under extreme pCO_2 compared to present day pCO_2 ($p < 0.001$).

Effects of temperature and pCO_2 stress on host energy reserves

Elevated temperatures significantly reduced *S. siderea* protein concentrations relative to corals in control temperatures ($p = 0.009$; Fig. 4a). Regardless of pCO_2 and temperature

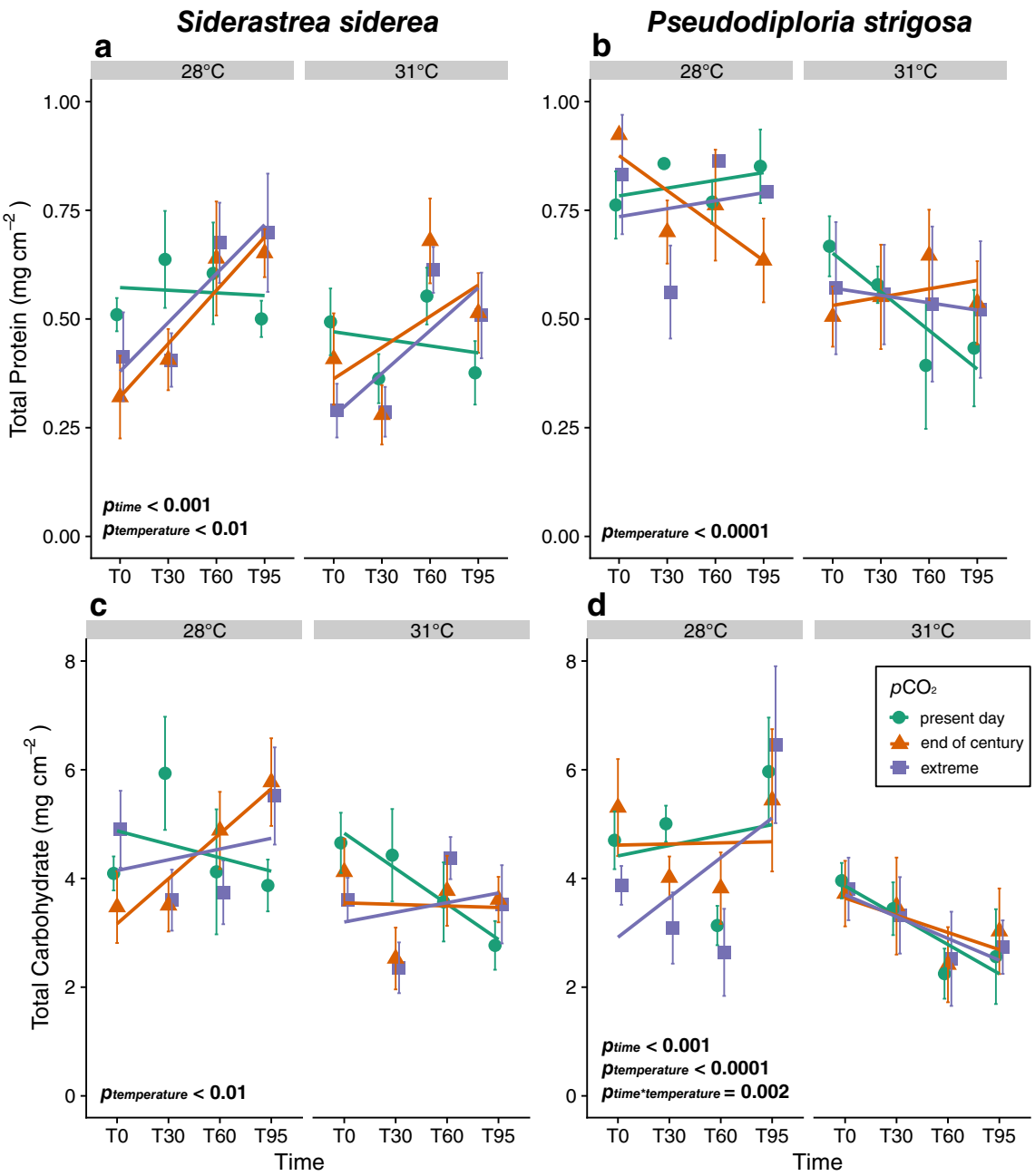

Fig. 4. Host energy reserves (total protein [**a**,**b**] and total carbohydrate [**c**, **d**]) of *Siderastrea siderea* (**a**, **c**) and *Pseudodiploria strigosa* (**b**, **d**) across four experimental durations (day 0 = T_0; day 30 [short-term] = T_{30}; day 60 [moderate-term] = T_{60}; day 95 [long-term] = T_{95}). Within panels, results are faceted by temperature and colored by pCO_2 (present day = green, end of century = orange, extreme = purple). Each point is an average of nearshore and forereef corals, with n = 4–6 (*S. siderea*) and n = 3–6 (*P. strigosa*) distinct fragments (n = 1/genotype). Significant factors are indicated in each panel. Lines represent linear fits (using ggplot2 *stat_smooth()* method to visualize differences regardless of model) for each treatment through time, and error bars represent standard error.

treatments, *S. siderea* proteins increased through time, and at T_{95} corals had higher mean protein than T_0 (p = 0.03). Neither pCO_2 nor reef zone significantly altered *S. siderea* protein concentrations. Similar to proteins, elevated temperatures significantly reduced *S. siderea* carbohydrate concentrations relative to control temperatures (Fig. 4c; p = 0.004). Neither pCO_2, reef zone, nor experiment duration significantly altered *S. siderea* carbohydrate concentrations.

Temperature significantly influenced *P. strigosa* protein (p < 0.001; Fig. 4b), with reduced protein concentrations under elevated temperatures compared to controls (p < 0.001). Neither pCO_2, reef zone, nor experiment duration

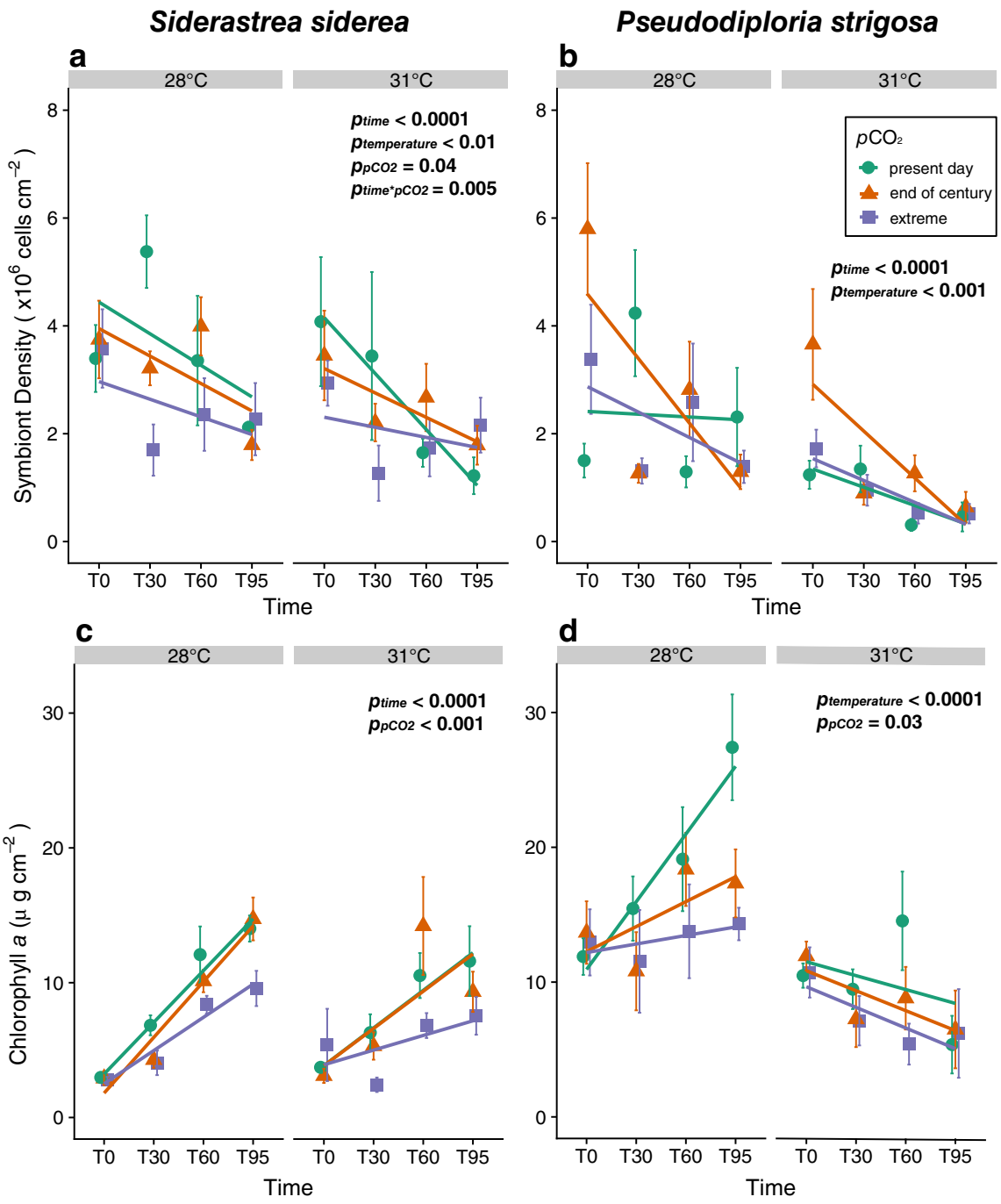

Fig. 5. Symbiodiniaceae physiology (symbiont cell density [**a**, **b**] and Chl *a* concentration [**c**, **d**]) of *Siderastrea siderea* (**a**, **c**) and *Pseudodiploria strigosa* (**b**, **d**) across four experimental durations (day 0 = T_0; day 30 [short-term] = T_{30}; day 60 [moderate-term] = T_{60}; day 95 [long-term] = T_{95}). Within panels, results are faceted by temperature and colored by pCO_2 (present day = green, end of century = orange, extreme = purple). Each point is an average of nearshore and forereef corals, with $n = 4$–6 (*S. siderea*) and $n = 3$–6 (*P. strigosa*) distinct fragments ($n = 1$/genotype). Significant factors are indicated in each panel. Lines represent linear fits (using ggplot2 *stat_smooth()* method to visualize differences regardless of model) for each treatment through time, and error bars represent standard error.

significantly altered *P. strigosa* protein concentrations. Similarly, *P. strigosa* total carbohydrate was reduced under elevated temperatures compared to control conditions ($p < 0.001$; Fig. 4d). Regardless of treatment, carbohydrates decreased between T_0 and T_{60} ($p < 0.01$). Under control temperatures, *P. strigosa* carbohydrates increased between T_{60} and T_{95} ($p = 0.004$); however, under elevated temperatures, carbohydrates did not increase significantly between T_{60} and T_{95}

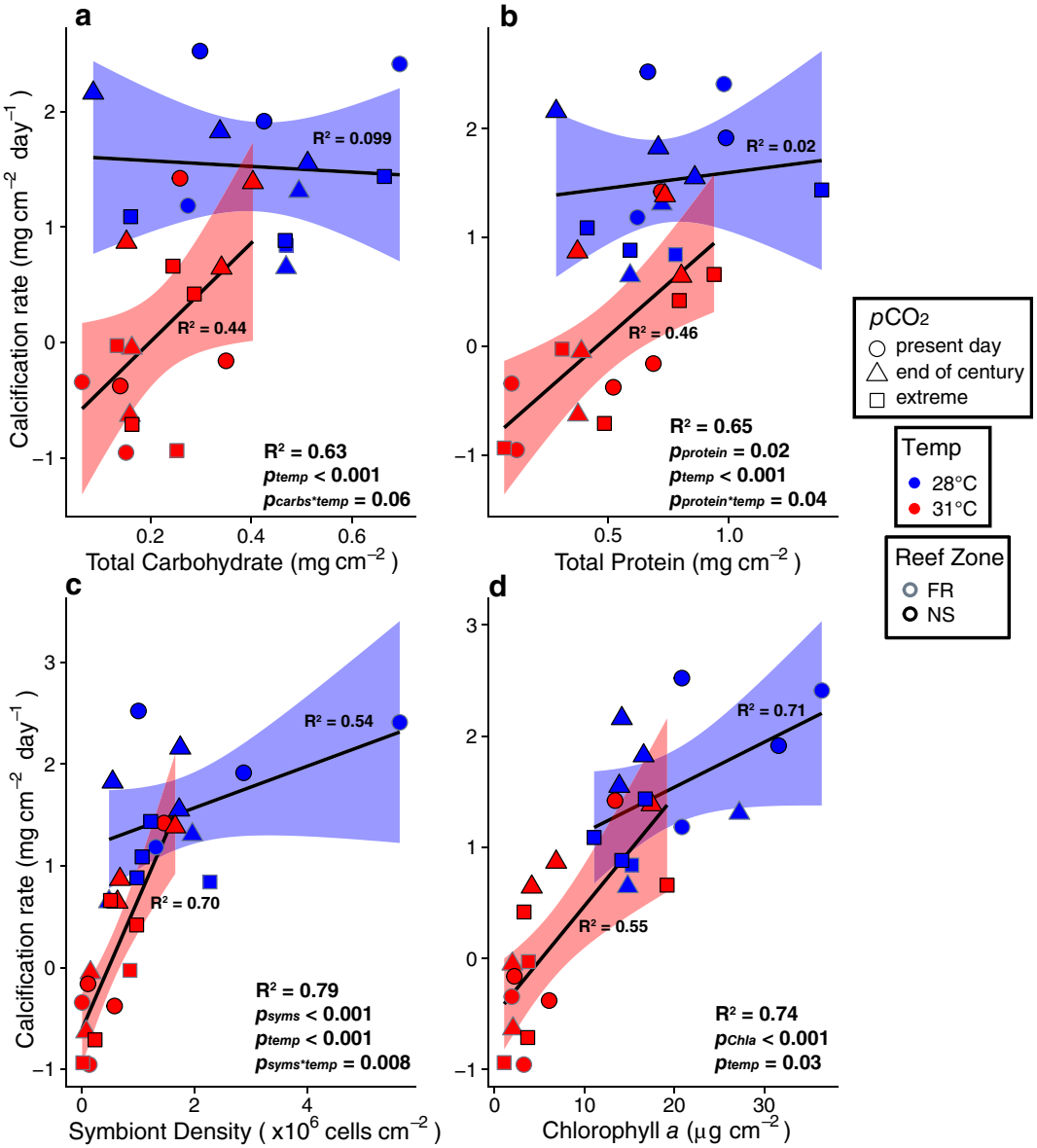

Fig. 6. Correlations of *Pseudodiploria strigosa* calcification rate with carbohydrates (**a**), proteins (**b**), symbiont density (**c**), and chlorophyll *a* (**d**) after long-term exposure to experimental treatments (T_{95}). Colors represent temperature treatment (red = 31°C, blue = 28°C), shapes represent pCO_2 (circle = present day, triangle = end of century, square = extreme), and shape outline colors represent reef zone (gray = forereef [FR], black = nearshore [NS]). Points represent individual coral fragments. Significant factors are indicated within each panel. Lines represent linear models of measured parameters within treatment through time, fit using ggplot2's *stat_smooth()* method with gray shading representing 95% confidence intervals for each temperature. Conditional R^2 values (Nakagawa and Schielzeth 2013) are reported for the whole model (bottom right corner of each facet) and for each temperature (next to the line of best fit).

(Fig. 4d). Neither pCO_2 nor reef zone significantly altered *P. strigosa* carbohydrate concentrations.

Effects of temperature and pCO_2 stress on symbiont physiology

Siderastrea siderea symbiont densities decreased from T_0 to T_{95} ($p = 0.0001$), were reduced under elevated temperatures compared to control ($p = 0.001$), and were reduced under extreme pCO_2 relative to end of century ($p = 0.04$; Fig. 5a). Reef zone did not significantly alter *S. siderea* symbiont densities. In contrast to symbiont density, *S. siderea* Chl *a* increased from T_0 to T_{95} ($p < 0.001$; Fig. 5c). Although corals under present day and end of century pCO_2 treatments exhibited similar Chl *a* concentrations, corals under extreme pCO_2 had significantly less Chl *a* compared to those under both present day ($p = 0.001$) and end of century ($p = 0.03$)

pCO_2. Neither reef zone nor temperature significantly altered *S. siderea* Chl *a*.

Regardless of pCO_2 treatment, *P. strigosa* had reduced symbiont densities under elevated temperatures compared to control temperatures ($p < 0.001$; Fig. 5b). Additionally, *P. strigosa* symbiont density was reduced at T_{95} relative to T_0 ($p < 0.001$). Neither pCO_2 nor reef zone significantly altered *P. strigosa* symbiont densities. Similarly, *P. strigosa* exhibited reduced Chl *a* under elevated temperatures compared to controls, regardless of pCO_2 treatment ($p < 0.001$; Fig. 5d). Additionally, *P. strigosa* Chl *a* was reduced under extreme pCO_2 compared to present day pCO_2 treatment regardless of temperature ($p = 0.02$). Neither reef zone nor experiment duration significantly altered *P. strigosa* Chl *a*.

Pseudodiploria strigosa physiological trait correlations

Pseudodiploria strigosa calcification rates were significantly correlated with all other physiological parameters ($p < 0.05$) after long-term exposure (T_{95}; Fig. S4), and temperature had a main effect on relationships between calcification and all other predictor variables (Fig. 6). Under elevated temperatures at T_{95}, *P. strigosa* fragments with higher protein ($p = 0.04$) and symbiont densities ($p = 0.001$) maintained faster calcification rates (Fig. 6b,c). A similar trend was observed for carbohydrates ($p = 0.06$; Fig. 6a). The interactive effect of temperature and the predictor variables on *P. strigosa* calcification rate was not significant until the end of the experiment (T_{95}; Fig. S5). Correlations for *Pseudodiploria strigosa* (Fig. 6) are presented in terms of temperature because it had a significant main effect on *P. strigosa* holobiont physiology at T_{95} (Fig. 2f). *Siderastrea siderea* correlation matrix (Fig. S4) and linear regression analyses did not reveal any significant interactions with treatment.

Discussion

Divergent responses of coral species to warming and acidification

Siderastrea siderea and *P. strigosa* exhibited divergent responses to two co-occurring global change stressors—ocean warming and acidification—and these responses were modulated by exposure duration. Overall *S. siderea* physiological performance was more negatively affected by acidification through time, while temperature had a more negative effect on *P. strigosa* over time. Such species-specific responses to temperature and acidification are not uncommon in reef-building corals. For example, when testing how 12 Caribbean coral species responded to crossed temperature and acidification conditions, Okazaki et al. (2017) observed that some species exhibited no growth response to either stressor (including *S. siderea* and *P. strigosa*), while other, more abundant species (e.g., *Orbicella faveolata* and *P. astreoides*), decreased calcification under both stressors. The difference between our findings and Okazaki et al. (2017) may be due to experiment duration (>30 d longer than Okazaki et al. 2017) or be the result of the more extreme treatments used here (31°C and ~3109 μatm compared to 30.3°C and 1300 μatm pCO_2). It is also possible that *S. siderea* and *P. strigosa* populations in Florida (Okazaki et al. 2017) could be less susceptible to stress than populations from the Belize MBRS studied here. For example, according to the climate variability hypothesis (Stevens 1989), higher latitude populations (e.g., Florida) that experience more variable thermal regimes (i.e., stronger seasonality) are predicted to be more phenotypically flexible and exhibit a wider range of thermal tolerances compared to populations closer to the equator (e.g., MBRS). A meta-analysis of Caribbean coral calcification responses to acidification, elevated temperature, and their combination found similar regional differences in stress responses between corals from Florida and Belize (Bove et al. 2020). While calcification of Florida corals did not clearly respond to acidification, elevated temperature, or their combination, elevated temperature reduced calcification rates in Belize corals (Bove et al. 2020). While acknowledging differences in annual temperature variability, Bove et al. (2020) highlight differences in experimental treatment extremes as the main driver of calcification. Although consideration of treatment level is critical, such population-level differences in stress tolerance have been previously observed in corals (Dixon et al. 2015). Interestingly, such population-level differences—specifically with respect to thermal tolerance and coral bleaching—do not appear to be related to history of pCO_2 exposure (Noonan and Fabricius 2016; Wall et al. 2018). Regardless, our results contribute to a growing body of literature supporting the resistance of *S. siderea* to elevated temperature and acidification (Castillo et al. 2014; Banks and Foster 2016; Davies et al. 2016; Bove et al. 2019).

Resistance of *S. siderea* to global change stressors was previously reported by Castillo et al. (2014), which found that only the most extreme temperature (32°C) and acidification (2553 μatm pCO_2) treatments reduced calcification rates. Castillo et al. (2014) concluded that *S. siderea* will be more negatively impacted by elevated temperatures over the coming century, given the IPCC's next-century acidification projections did not reduce calcification. Our findings are consistent with this work, as only extreme—but not end of century pCO_2—reduced *S. siderea* calcification. Gene expression profiling of *S. siderea* from the Castillo et al. (2014) coral fragments revealed that thermal stress caused large-scale downregulation of gene expression, while acidification elicited upregulation of proton transport genes (Davies et al. 2016). This potentially offsets effects of acidification at the site of calcification (e.g., Ries 2011), although this is potentially complicated by the electrochemical challenges of exporting H^+ from the calcifying fluid under acidified conditions (proton flux hypothesis; Jokiel 2011). These findings provide further support for *S. siderea*'s ability to acclimate to acidification.

Bove et al. (2019) investigated the combined effects of similar temperature and acidification treatments on four coral

species: *S. siderea*, *P. strigosa*, *P. astreoides*, and *Undaria tenuifolia*. After 93 d, calcification declined in all species under increased pCO_2. However, only *P. strigosa* reduced calcification under elevated temperature, which is consistent with results presented here and highlights that thermal stress more negatively impacts *P. strigosa* than *S. siderea* (Fig. 2d–f). Additionally, Bove et al. (2019) found that *S. siderea* was the most resistant of the four species, and maintained positive calcification rates even in the most extreme acidification treatment (~3300 μatm pCO_2)—findings that are also corroborated here (Fig. 3a). By quantifying net calcification rates at 30-d increments, we show that *S. siderea* net calcification was negative under extreme pCO_2 at T_{60}, but that rates recovered by T_{95} (Fig. 3a). This result is potentially due to acclimation to stressful conditions over time, perhaps through transcriptome plasticity, as previously proposed in *S. siderea* (Davies et al. 2016) and in *P. astreoides* (Kenkel and Matz 2016); however, without following these colonies for even longer time periods, it is impossible to know without follow-up experimental work.

Stress differentially modulates physiology across coral species

Under thermal and acidification stress, corals can draw on energy reserves, including lipids, proteins, and carbohydrates, to maintain and/or produce tissue and skeleton (Anthony et al. 2009; Schoepf et al. 2013). In addition to using energetic reserves, heterotrophy (Towle et al. 2015; Aichelman et al. 2016) or enhanced productivity of Symbiodiniaceae owing to CO_2 fertilization of photosynthesis (Brading et al. 2011) can augment energetic resources in zooxanthellate corals. Coral energetic reserves can therefore influence resistance to and recovery from thermal stress (Grottoli et al. 2006; Grottoli et al. 2014) as well as resistance to acidification (Wall et al. 2017).

In this study, host energy reserves of *S. siderea* and *P. strigosa* responded to temperature and acidification stress in different ways. Between T_0 and T_{60}, *P. strigosa* exhibited reduced carbohydrates regardless of treatment, indicating catabolism of this energy reserve (Fig. 4d). This was followed by restoration of carbohydrates (acclimation) at control temperatures at T_{95} (Fig. 4d), which likely supported the positive calcification rates also observed under these conditions (Fig. 6a, S5). Protein reserves did not emulate trends in carbohydrates (Fig. 4b), potentially owing to *P. strigosa* catabolizing carbohydrates before proteins, which has been observed over shorter time scales in other scleractinian corals (Grottoli et al. 2004). This sequence of energy reserve catabolism is consistent with relative enthalpies of combustion: carbohydrates are considered a short-term energy source and have the lowest enthalpy of combustion, lipids are a longer-term energy source and have the highest enthalpy of combustion, and proteins are intermediate (Gnaiger and Bitterlich 1984; Grottoli et al. 2004). Elevated protein reserves did predict faster calcification rates in *P. strigosa* under elevated temperatures, but only after long-term exposure (Fig. 6b, S5). As photosynthate translocated from symbionts is a major source of carbohydrates to coral hosts (Burriesci et al. 2012), reductions in *P. strigosa* symbiont densities, Chl *a*, and carbohydrates at elevated temperature suggests that symbionts were translocating fewer resources to the host, which likely contributed to reductions in calcification under elevated temperatures, particularly after long-term exposure (T_{95}; Fig. 6, S5). Total protein and carbohydrate of *S. siderea*, similar to *P. strigosa*, declined under elevated temperatures (Fig. 4a,c)—consistent with previous work highlighting upregulation of protein catabolism pathways in *S. siderea* exposed to long-term thermal stress (Davies et al. 2016). Grottoli et al. (2004) previously linked species-level differences in energy catabolism to differences in photosynthesis/respiration ratios, and while we did not explore these traits here, this would be a worthy pursuit for future studies to better contextualize energy reserve catabolism of *S. siderea* and *P. strigosa* under stress. Additionally, a limitation to the present study is that lipid content was not measured through time, thereby precluding evaluation of a potential contributor to energy reserve catabolism under stress, as Wall et al. (2017) observed for *Pocillopora acuta*.

An overall trend in reduced symbiont density and increased Chl *a* through time was observed under most pCO_2 and temperature conditions, except for *P. strigosa* under elevated temperature (Fig. 5). Given that both species under most treatments exhibited this pattern, it cannot be ruled out that these changes in symbiont physiology were influenced by other factors, including incomplete symbiont acclimation to experimental light environment (Roth 2014) and seasonal patterns in symbiont density and pigment concentration (Fitt et al. 2000)—which may have masked the symbiont response to thermal stress within *S. siderea*. In contrast, *P. strigosa* exhibited reduced symbiont density and Chl *a* under elevated temperature (Fig. 5b,d), a pattern more consistent with thermally induced bleaching (Weis 2008) and further illustrating the susceptibility of this species to thermal stress.

Nearshore *P. strigosa* are more resistant than forereef conspecifics

Reef zone was a significant predictor of host physiology, particularly for *P. strigosa*, as nearshore corals exhibited greater net calcification (Fig. 3b). Although reef zone differences in calcification were observed for *S. siderea* (particularly through time), corals from one reef zone did not clearly outperform the other. In contrast, reef zone-specific calcification of *P. strigosa* may arise from local adaptation of the host to distinct temperature regimes. The Belize MBRS nearshore habitats have higher maximum temperatures, greater annual temperature range, and more days above the regional thermal bleaching threshold compared to forereef sites (Baumann et al. 2016). Local adaptation to distinct reef zones is not uncommon in corals and has been previously shown to affect coral responses to thermal stress. For example, *P. astreoides*

was locally adapted to distinct thermal regimes in Florida, with inshore corals exhibiting higher thermal tolerance, constitutively higher expression of specific metabolic genes, and greater gene expression plasticity compared to offshore conspecifics (Kenkel et al. 2013*a*; Kenkel et al. 2013*b*; Kenkel and Matz 2016). A similar pattern of local adaptation was previously suggested for three Hawaiian coral species native to the warmer and more acidic Kāne'ohe Bay, as corals were more tolerant to experimental temperature and pCO_2 stress relative to conspecifics from a cooler and less acidic site (Jury and Toonen 2019).

Pseudodiploria strigosa is a hermaphroditic broadcast spawning species, and previous work on the Flower Garden Banks population demonstrated that these larvae have short pelagic durations compared with other broadcast spawning scleractinian corals (e.g., *Orbicella franksi*), which could facilitate local adaptation as larvae are more likely to recruit locally (Davies et al. 2017). However, it is unknown if *P. strigosa* on the Belize MBRS have similarly short pelagic larval durations. We hypothesize that nearshore *P. strigosa* are locally adapted and/or acclimated to more variable and stressful nearshore conditions, allowing maintenance of higher calcification rates under thermal stress compared to their forereef counterparts. However, responses based on reef zone could be obscured by uneven sampling across sites, as forereef genotypes of *P. strigosa* were underrepresented in the experiment (2 genotypes vs. the standard 3) due to mortality of one forereef colony before the experiment began. We do acknowledge, however, that greater replication within each site may have yielded different effects of reef zone in other parameters of *P. strigosa* physiology due to the well documented additive genetic variation within coral populations (Dixon et al. 2015; Kavousi et al. 2016).

Time-course experiments reveal acclimation to thermal stress

This study contributes to a growing body of literature demonstrating the value of assessing time-course physiology of corals under stress. Although studies investigating independent effects of temperature and acidification on corals have yielded insight into the effects of global change (e.g., Jokiel and Coles 1990; Albright et al. 2018), combined effects of these stressors remain less explored—particularly in the context of how coral stress is modulated by stress duration. By characterizing host and symbiont physiology of the same colony through time, acclimatory responses were identified in two coral species, providing further evidence of the species-specific nature of coral acclimation. For example, under extreme pCO_2 and elevated temperature, *S. siderea* net calcification appears to recover by the end of the experiment while *P. strigosa* calcification continues to decline with time, resulting in negative net calcification by T_{95}. Notably, these results would not have been apparent in shorter-term exposures. Additionally, the exposure duration component of this study suggests that species will exhibit differential responses to ephemeral stress events. Local heat waves that raise SST and upwelling events that reduce pH—factors that already threaten coral populations—may threaten coral species in different ways in the future depending on the duration of these events. The lack of a statistical difference in pCO_2 levels between several of the treatments at T_0 (end of century pCO_2 treatment at 31°C was lower than target pCO_2; Fig. S2) may have also affected the corals' physiological response through time. It is possible that if corals in this end of century, 31°C treatment had been exposed to the target pCO_2 for longer, additional physiological responses through time would have been observed. However, this does not negate the key findings that *P. strigosa* was most responsive to elevated temperature while *S. siderea* was most responsive to extreme pCO_2. Additionally, the goal of this study was to characterize how corals acclimate to global change stressors through time, and the observed responses to treatments relevant to predicted future ocean conditions—particularly *P. strigosa* in response to temperature—highlights that exposure to these conditions is likely not sustainable over the course of the lifespans of individuals of this species. Interestingly, our results suggest that such stress exposure could be more sustainable for *S. siderea*.

Acclimation is an important mechanism by which corals can withstand changing environmental conditions, and transcriptome plasticity is one way that corals can acclimate to stress (Davies et al. 2016; Kenkel and Matz 2016; Rivera et al. 2021). For example, a coral reciprocal transplant experiment revealed that adaptive gene expression plasticity of stress response genes was associated with reduced susceptibility to bleaching (Kenkel and Matz 2016). In addition to plasticity providing a mechanism for acclimation within a generation, corals can rapidly adapt through selection on standing genetic variation in thermal tolerance traits (Dixon et al. 2015; Matz et al. 2018). However, recent declines in coral abundance, diversity, and health suggest rates of intra- and trans-generational adaptation to global change stressors within most coral populations are insufficient for mitigating deleterious impacts of global change (Thomas et al. 2018). Additionally, in contrast to the demonstrated importance of gene expression plasticity in acclimating to different temperature environments, Comeau et al. (2019) demonstrated that corals were unable to acclimatize to acidification conditions by altering calcifying fluid chemistry over the course of 1 yr. Understanding the interplay of acclimation and adaptation in scleractinian corals is therefore essential for projecting how corals will fare in the higher-CO_2 future. Studies focusing on long-term acclimation capacities of corals will further elucidate mechanisms of resistance and resilience to global stressors.

References

Agostini, S., and others. 2013. The effects of thermal and high-CO_2 stresses on the metabolism and surrounding

microenvironment of the coral *Galaxea fascicularis*. C. R. Biol. **336**: 384–391. doi:10.1016/j.crvi.2013.07.003

Aichelman, H. E., J. E. Townsend, T. A. Courtney, J. H. Baumann, S. W. Davies, and K. D. Castillo. 2016. Heterotrophy mitigates the response of the temperate coral *Oculina arbuscula* to temperature stress. Ecol. Evol. **6**: 6758–6769. doi:10.1002/ece3.2399

Albright, R., and others. 2018. Carbon dioxide addition to coral reef waters suppresses net community calcification. Nature **555**: 516. doi:10.1038/nature25968

Anderson, K. D., N. E. Cantin, J. M. Casey, and M. S. Pratchett. 2019. Independent effects of ocean warming versus acidification on the growth, survivorship and physiology of two *Acropora* corals. Coral Reefs **38**: 1225–1240. doi:10.1007/s00338-019-01864-y

Anthony, K. R., M. O. Hoogenboom, J. A. Maynard, A. G. Grottoli, and R. Middlebrook. 2009. Energetics approach to predicting mortality risk from environmental stress: A case study of coral bleaching. Funct. Ecol. **23**: 539–550. doi:10.1111/j.1365-2435.2008.01531.x

Banks, S., and K. Foster. 2016. Baseline levels of *Siderastrea siderea* bleaching under normal environmental conditions in little Cayman. Open J. Mar. Sci. **7**: 142–154. doi:10.4236/ojms.2017.71011

Baumann, J. H., and others. 2016. Temperature regimes impact coral assemblages along environmental gradients on lagoonal reefs in Belize. PloS One **11**: e0162098. doi:10.1371/journal.pone.0162098

Bay, R. A., and S. R. Palumbi. 2014. Multilocus adaptation associated with heat resistance in reef-building corals. Curr. Biol. **24**: 2952–2956. doi:10.1016/j.cub.2014.10.044

Bove, C., J. Umbanhowar, and K. D. Castillo. 2020. Meta-analysis reveals reduced coral calcification under projected ocean warming but not under acidification across the Caribbean Sea. Front. Mar. Sci. **7**: 127. doi:10.3389/fmars.2020.00127

Bove, C. B., J. B. Ries, S. W. Davies, I. T. Westfield, J. Umbanhowar, and K. D. Castillo. 2019. Common Caribbean corals exhibit highly variable responses to future acidification and warming. Proc. R. Soc. B **286**: 20182840. doi:10.1098/rspb.2018.2840

Brading, P., M. E. Warner, P. Davey, D. J. Smith, E. P. Achterberg, and D. J. Suggett. 2011. Differential effects of ocean acidification on growth and photosynthesis among phylotypes of Symbiodinium (Dinophyceae). Limnol. Oceanogr. **56**: 927–938. doi:10.4319/lo.2011.56.3.0927

Burriesci, M. S., T. K. Raab, and J. R. Pringle. 2012. Evidence that glucose is the major transferred metabolite in dinoflagellate–cnidarian symbiosis. J. Exp. Biol. **215**: 3467–3477. doi:10.1242/jeb.070946

Castillo, K. D., J. B. Ries, J. F. Bruno, and I. T. Westfield. 2014. The reef-building coral *Siderastrea siderea* exhibits parabolic responses to ocean acidification and warming. Proc. R. Soc. B **281**: 20141856. doi:10.1098/rspb.2014.1856

Castillo, K. D., J. B. Ries, J. M. Weiss, and F. P. Lima. 2012. Decline of forereef corals in response to recent warming linked to history of thermal exposure. Nat. Clim. Change. **2**: 756. doi:10.1038/nclimate1577

Comeau, S., C. Cornwall, T. DeCarlo, S. Doo, R. Carpenter, and M. McCulloch. 2019. Resistance to ocean acidification in coral reef taxa is not gained by acclimatization. Nat. Clim. Change **9**: 477. doi:10.1038/s41558-019-0486-9

Costanza, R., and others. 2014. Changes in the global value of ecosystem services. Global Environ. Change **26**: 152–158. doi:10.1016/j.gloenvcha.2014.04.002

Davies, P. S. 1989. Short-term growth measurements of corals using an accurate buoyant weighing technique. Mar. Biol. **101**: 389–395. doi:10.1007/BF00428135

Davies, S. W., A. Marchetti, J. B. Ries, and K. D. Castillo. 2016. Thermal and pCO_2 stress elicit divergent transcriptomic responses in a resilient coral. Front. Mar. Sci. **3**: 112. doi:10.3389/fmars.2016.00112

Davies, S. W., M. E. Strader, J. T. Kool, C. D. Kenkel, and M. V. Matz. 2017. Modeled differences of coral life-history traits influence the refugium potential of a remote Caribbean reef. Coral Reefs **36**: 913–925. doi:10.1007/s00338-017-1583-8

Dixon, G. B., S. W. Davies, G. V. Aglyamova, E. Meyer, L. K. Bay, and M. V. Matz. 2015. Genomic determinants of coral heat tolerance across latitudes. Science **348**: 1460–1462. doi:10.1126/science.1261224

Doney, S. C., V. J. Fabry, R. A. Feely, and J. A. Kleypas. 2009. Ocean acidification: The other CO2 problem. Ann. Rev. Mar. Sci. **1**: 169–192. doi:10.1146/annurev.marine.010908.163834

Edmunds, P. J. 2005. The effect of sub-lethal increases in temperature on the growth and population trajectories of three scleractinian corals on the southern Great Barrier Reef. Oecologia **146**: 350–364. doi:10.1007/s00442-005-0210-5

Edmunds, P. J., D. Brown, and V. Moriarty. 2012. Interactive effects of ocean acidification and temperature on two scleractinian corals from Moorea, French Polynesia. Global Change Biol. **18**: 2173–2183. doi:10.1111/j.1365-2486.2012.02695.x

Fitt, W. K., F. McFarland, M. E. Warner, and G. C. Chilcoat. 2000. Seasonal patterns of tissue biomass and densities of symbiotic dinoflagellates in reef corals and relation to coral bleaching. Limnol. Oceanogr. **45**: 677–685. doi:10.4319/lo.2000.45.3.0677

Gnaiger, E., and G. Bitterlich. 1984. Proximate biochemical composition and caloric content calculated from elemental CHN analysis: A stoichiometric concept. Oecologia **62**: 289–298. doi:10.1007/BF00384259

Grottoli, A., L. Rodrigues, and C. Juarez. 2004. Lipids and stable carbon isotopes in two species of Hawaiian corals, *Porites compressa* and *Montipora verrucosa*, following a bleaching event. Mar. Biol. **145**: 621–631. doi:10.1007/s00227-004-1337-3

Grottoli, A. G., L. J. Rodrigues, and J. E. Palardy. 2006. Heterotrophic plasticity and resilience in bleached corals. Nature **440**: 1186. doi:10.1038/nature04565

Grottoli, A. G., and others. 2014. The cumulative impact of annual coral bleaching can turn some coral species winners into losers. Glob. Chang. Biol. **20**: 3823–3833. doi:10.1111/gcb.12658

Guillermic, M., and others. 2021. Thermal stress reduces pocilloporid coral resilience to ocean acidification by impairing control over calcifying fluid chemistry. Sci. Adv. **7**: eaba9958. doi:10.1126/sciadv.aba9958

Hoegh-Guldberg, O., P. J. Mumby, A. J. Hooten, R. S. Steneck, P. Greenfield, E. Gomez, C. D. Harvell, P. F. Sale, A. J. Edwards, and K. Caldeira. 2007. Coral reefs under rapid climate change and ocean acidification. Science. **318**: 1737–1742.

Holcomb, M., A. L. Cohen, and D. C. McCorkle. 2012. An investigation of the calcification response of the scleractinian coral *Astrangia poculata* to elevated pCO2 and the effects of nutrients, zooxanthellae and gender. Biogeosciences **9**: 29–39. doi:10.5194/bg-9-29-2012

Horvath, K. M., K. D. Castillo, P. Armstrong, I. T. Westfield, T. Courtney, and J. B. Ries. 2016. Next-century ocean acidification and warming both reduce calcification rate, but only acidification alters skeletal morphology of reef-building coral *Siderastrea siderea*. Sci. Rep. **6**: 29613. doi:10.1038/srep29613

Hughes, T. P., and others. 2017. Global warming and recurrent mass bleaching of corals. Nature **543**: 373. doi:10.1038/nature21707

Jokiel, P., and S. Coles. 1990. Response of Hawaiian and other Indo-Pacific reef corals to elevated temperature. Coral Reefs **8**: 155–162. doi:10.1007/BF00265006

Jokiel, P. L. 2011. Ocean acidification and control of reef coral calcification by boundary layer limitation of proton flux. Bull. Mar. Sci. **87**: 639–657. doi:10.5343/bms.2010.1107

Jury, C. P., and R. J. Toonen. 2019. Adaptive responses and local stressor mitigation drive coral resilience in warmer, more acidic oceans. Proc. R. Soc. B **286**: 20190614. doi:10.1098/rspb.2019.0614

Kavousi, J., Y. Tanaka, K. Nishida, A. Suzuki, Y. Nojiri, and T. Nakamura. 2016. Colony-specific calcification and mortality under ocean acidification in the branching coral *Montipora digitata*. Mar. Environ. Res. **119**: 161–165. doi:10.1016/j.marenvres.2016.05.025

Kenkel, C., G. Goodbody-Gringley, D. Caillaud, S. Davies, E. Bartels, and M. Matz. 2013*a*. Evidence for a host role in thermotolerance divergence between populations of the mustard hill coral (*Porites astreoides*) from different reef environments. Mol. Ecol. **22**: 4335–4348. doi:10.1111/mec.12391

Kenkel, C., E. Meyer, and M. Matz. 2013*b*. Gene expression under chronic heat stress in populations of the mustard hill coral (*Porites astreoides*) from different thermal environments. Mol. Ecol. **22**: 4322–4334. doi:10.1111/mec.12390

Kenkel, C. D., and M. V. Matz. 2016. Gene expression plasticity as a mechanism of coral adaptation to a variable environment. Nat. Ecol. Evol. **1**: 0014. https://doi.org/10.1038/s41559-016-0014

Kline, D. I., and others. 2019. Living coral tissue slows skeletal dissolution related to ocean acidification. Nat. Ecol. Evol. **3**: 1438–1444. doi:10.1038/s41559-019-0988-x

Kornder, N. A., B. M. Riegl, and J. Figueiredo. 2018. Thresholds and drivers of coral calcification responses to climate change. Glob. Chang. Biol. **24**: 5084–5095. doi:10.1111/gcb.14431

Kroeker, K. J., and others. 2013. Impacts of ocean acidification on marine organisms: Quantifying sensitivities and interaction with warming. Glob. Chang. Biol. **19**: 1884–1896. doi:10.1111/gcb.12179

LaJeunesse, T. C., and others. 2018. Systematic revision of Symbiodiniaceae highlights the antiquity and diversity of coral endosymbionts. Curr. Biol. **28**: 2570–2580.e2576. doi:10.1016/j.cub.2018.07.008

Lê, S., J. Josse, and F. Husson. 2008. FactoMineR: An R package for multivariate analysis. J. Stat. Softw. **25**: 1–18.

Levas, S., V. Schoepf, M. E. Warner, M. Aschaffenburg, J. Baumann, and A. G. Grottoli. 2018. Long-term recovery of Caribbean corals from bleaching. J. Exp. Mar. Biol. Ecol. **506**: 124–134. doi:10.1016/j.jembe.2018.06.003

Liu, Y.-W., J. N. Sutton, J. B. Ries, and R. A. Eagle. 2020. Regulation of calcification site pH is a polyphyletic but not always governing response to ocean acidification. Sci. Adv. **6**: eaax1314. doi:10.1126/sciadv.aax1314

Marchetti, A., and others. 2012. Comparative metatranscriptomics identifies molecular bases for the physiological responses of phytoplankton to varying iron availability. Proc. Natl. Acad. Sci. **109**: E317–E325. doi:10.1073/pnas.1118408109

Masuko, T., A. Minami, N. Iwasaki, T. Majima, S.-I. Nishimura, and Y. C. Lee. 2005. Carbohydrate analysis by a phenol–sulfuric acid method in microplate format. Anal. Biochem. **339**: 69–72. doi:10.1016/j.ab.2004.12.001

Matz, M. V., E. A. Treml, G. V. Aglyamova, and L. K. Bay. 2018. Potential and limits for rapid genetic adaptation to warming in a Great Barrier Reef coral. PLoS Genet. **14**: e1007220. doi:10.1371/journal.pgen.1007220

McLachlan, R. H., J. T. Price, S. L. Solomon, and A. G. Grottoli. 2020. Thirty years of coral heat-stress experiments: A review of methods. Coral Reefs. **39**: 885–902. doi:10.1007/s00338-020-01931-9

Morley, J. W., R. L. Selden, R. J. Latour, T. L. Frölicher, R. J. Seagraves, and M. L. Pinsky. 2018. Projecting shifts in thermal habitat for 686 species on the North American continental shelf. PloS One **13**: e0196127. doi:10.1371/journal.pone.0196127

Mucci, A. 1983. The solubility of calcite and aragonite in seawater at various salinities, temperatures, and one

atmosphere total pressure. Am. J. Sci. **283**: 780–799. doi:10.2475/ajs.283.7.780

Nakagawa, S., and H. Schielzeth. 2013. A general and simple method for obtaining R2 from generalized linear mixed-effects models. Methods Ecol. Evol. **4**: 133–142. doi:10.1111/j.2041-210x.2012.00261.x

Noonan, S. H., and K. E. Fabricius. 2016. Ocean acidification affects productivity but not the severity of thermal bleaching in some tropical corals. ICES J. Mar. Sci. **73**: 715–726. doi:10.1093/icesjms/fsv127

Okazaki, R. R., and others. 2017. Species-specific responses to climate change and community composition determine future calcification rates of Florida keys reefs. Glob. Chang. Biol. **23**: 1023–1035. doi:10.1111/gcb.13481

Oksanen, J., F. Guillaume Blanchet, M. Friendly, R. Kindt, P. Legendre, D. McGlinn, P. R., Minchin, R. B. O'Hara, G. L., Simpson, P. Solymos, M. H. H. Stevens, Eduard Szoecs and Helene Wagner (2020). vegan: Community Ecology Package. R package version 2.5-7. https://CRAN.R-project.org/package=vegan.

Pierrot, D., E. Lewis, and D. Wallace. 2006. MS Excel program developed for CO2 system calculations. ORNL/CDIAC-105a. Oak Ridge, TN: Carbon Dioxide Information Analysis Center, Oak Ridge National Laboratory, US Department of Energy.

Pörtner, H., and others. 2019. IPCC special report on the ocean and cryosphere in a changing climate. Geneva: IPCC Intergovernmental Panel on Climate Change.

R Core Team. 2017. R: A language and environment for statistical computing. R Foundation for Statistical Computing, Vienna, Austria. https://www.R-project.org/.

Reynaud, S., N. Leclercq, S. Romaine-Lioud, C. Ferrier-Pagés, J. Jaubert, and J. P. Gattuso. 2003. Interacting effects of CO2 partial pressure and temperature on photosynthesis and calcification in a scleractinian coral. Global Change Biology **9**: 1660–1668.

Ries, J., A. Cohen, and D. McCorkle. 2010. A nonlinear calcification response to CO2-induced ocean acidification by the coral Oculina arbuscula. Coral Reefs **29**: 661–664.

Ries, J. B. 2011. A physicochemical framework for interpreting the biological calcification response to CO2-induced ocean acidification. Geochim. Cosmochim. Acta **75**: 4053–4064. doi:10.1016/j.gca.2011.04.025

Rigby, R. A., and D. M. Stasinopoulos. 2005. Generalized additive models for location, scale and shape. J. Roy. Stat. Soc. Ser. C. (Appl. Stat.) **54**: 507–554. doi:10.1111/j.1467-9876.2005.00510.x

Rivera, H. E., and others. 2021. A framework for understanding gene expression plasticity and its influence on stress tolerance. Mol. Ecol. **30**: 1381–1397. doi:10.1111/mec.15820

Rodolfo-Metalpa, R., and others. 2011. Coral and mollusc resistance to ocean acidification adversely affected by warming. Nat. Clim. Change. **1**: 308. doi:10.1038/nclimate1200

Rodrigues, L. J., and A. G. Grottoli. 2007. Energy reserves and metabolism as indicators of coral recovery from bleaching. Limnol. Oceanogr. **52**: 1874–1882. doi:10.4319/lo.2007.52.5.1874

Roth, M. S. 2014. The engine of the reef: Photobiology of the coral–algal symbiosis. Front. Microbiol. **5**: 422. doi:10.3389/fmicb.2014.00422

Roy, R. N., and others. 1993. The dissociation constants of carbonic acid in seawater at salinities 5 to 45 and temperatures 0 to 45°C. Mar. Chem. **44**: 249–267. doi:10.1016/0304-4203(93)90207-5

Rueden, C. T., and others. 2017. ImageJ2: ImageJ for the next generation of scientific image data. BMC Bioinformatics **18**: 529. doi:10.1186/s12859-017-1934-z

Schoepf, V., and others. 2013. Coral energy reserves and calcification in a high-CO2 world at two temperatures. PloS One **8**: e75049. doi:10.1371/journal.pone.0075049

Stevens, G. C. 1989. The latitudinal gradient in geographical range: How so many species coexist in the tropics. Am. Nat. **133**: 240–256. doi:10.1086/284913

IPCC, 2013. Climate Change 2013: The Physical Science Basis. Contribution of Working Group I to the Fifth Assessment Report of the Intergovernmental Panel on Climate Change Stocker, T.F., D. Qin, G.-K. Plattner, M. Tignor, S.K. Allen, J. Boschung, A. Nauels, Y. Xia, V. Bex and P.M. Midgley (eds.). Cambridge University Press, Cambridge, United Kingdom and New York, NY, USA, 1535 pp.

Thomas, L., and others. 2018. Mechanisms of thermal tolerance in reef-building corals across a fine-grained environmental mosaic: Lessons from Ofu, American Samoa. Front. Mar. Sci. **4**: 434. doi:10.3389/fmars.2017.00434

Towle, E. K., I. C. Enochs, and C. Langdon. 2015. Threatened Caribbean coral is able to mitigate the adverse effects of ocean acidification on calcification by increasing feeding rate. PloS one **10**: e0123394. doi:10.1371/journal.pone.0123394

Van Vuuren, D. P., and others. 2011. The representative concentration pathways: An overview. Clim. Change **109**: 5. doi:10.1007/s10584-011-0148-z

Wall, C., R. Mason, W. Ellis, R. Cunning, and R. Gates. 2017. Elevated pCO2 affects tissue biomass composition, but not calcification, in a reef coral under two light regimes. R. Soc. Open Sci. **4**: 170683. doi:10.1098/rsos.170683

Wall, C. B., C. A. Ricci, G. E. Foulds, L. D. Mydlarz, R. D. Gates, and H. M. Putnam. 2018. The effects of environmental history and thermal stress on coral physiology and immunity. Mar. Biol. **165**: 56. doi:10.1007/s00227-018-3317-z

Weis, V. M. 2008. Cellular mechanisms of cnidarian bleaching: Stress causes the collapse of symbiosis. J. Exp. Biol. **211**: 3059–3066. doi:10.1242/jeb.009597

Acknowledgments

We thank the Belize Fisheries Department for coral collection permits. Isaac Westfield, Amanda Dwyer, Sara Williams, and Louise Cameron are acknowledged for assisting with experimental maintenance at Northeastern University. Thanks to the Marchetti and Septer labs at the University of North Carolina at Chapel Hill for assistance with equipment and lab space to complete physiological assays. We also thank Samir Patel, Savannah Swinea, Bailey Thomasson, Forrest Buckthal, and Cori Lopazanski for assisting with preparing corals for physiological assays. This work was supported by NSF award OCE-1437371 (to J.B.R.), NSF award OCE-1459522 (to K.D.C.), NOAA award NA13OAR4310186 (to J.B.R. and K.D.C.), and the National Academies of Sciences, Engineering, and Medicine Gulf Research Program Fellowship (to S.W.D.). H.E.A. was supported by the NSF Graduate Research Fellowships Program (2016222953) and S.W.D. was a Simons Foundation Fellow of the Life Sciences Research Foundation (LSRF) while completing part of this research.

Conflict of interest

None declared.

Submitted 27 July 2020
Revised 11 February 2021
Accepted 11 May 2021

Associate editor: Bradley Eyre